Polymer Chemistry

Accepted Manuscript

Volume 7 | Number 1 | 7 January 2016 | Pages 1–246

Polymer Chemistry

www.rsc.org/polymers

ISSN 1759-9954

ROYAL SOCIETY OF CHEMISTRY

PAPER
Munju Goh et al.
Enhancement of the crosslink density, glass transition temperature, and strength of epoxy resin by using functionalized graphene oxide co-curing agents

175 YEARS

This is an Accepted Manuscript, which has been through the Royal Society of Chemistry peer review process and has been accepted for publication.

Accepted Manuscripts are published online shortly after acceptance, before technical editing, formatting and proof reading. Using this free service, authors can make their results available to the community, in citable form, before we publish the edited article. We will replace this Accepted Manuscript with the edited and formatted Advance Article as soon as it is available.

You can find more information about Accepted Manuscripts in the author guidelines.

Please note that technical editing may introduce minor changes to the text and/or graphics, which may alter content. The journal's standard Terms & Conditions and the ethical guidelines, outlined in our author and reviewer resource centre, still apply. In no event shall the Royal Society of Chemistry be held responsible for any errors or omissions in this Accepted Manuscript or any consequences arising from the use of any information it contains.

ROYAL SOCIETY OF CHEMISTRY

rsc.li/polymers

Journal Name

ARTICLE

Towards bio-based tapered block copolymers: the behaviour of myrcene in the statistical anionic copolymerisation

Eduard Grune,[a,b] Jennifer Bareuther,[c] Jan Blankenburg,[a,b] Michael Appold,[c] Lloyd Shaw,[d] Axel H. E. Müller,[a] George Floudas,[e,f] Lian R. Hutchings,*[d] Markus Gallei*[c] and Holger Frey *,[a]

To explore the potential of myrcene (Myr) as a bio-based monoterpene comonomer for styrenic copolymers and to establish its general applicability for the carbanionic copolymerisation, several statistical copolymerisations of myrcene and common monomers like isoprene (I), styrene (S) and 4-methylstyrene (4MS) were carried out in cyclohexane and monitored by *in situ* ^{1}H NMR spectroscopy. Real-time NMR kinetic studies permitted the determination of the reactivity ratios and the composition profile for each monomer combination. While the copolymerisation of Myr/I yielded a gradient copolymer and reactivity ratios of moderate disparity (r_{Myr} = 4.4; r_I = 0.23), the statistical copolymerisation of Myr/S and Myr/4MS afforded block-like, tapered copolymers due to highly diverging reactivity ratios (r_{Myr} = 36; r_S = 0.028 and r_{Myr} = 140; r_{4MS} = 0.0074). Furthermore, a terpolymerisation of Myr/I/4MS was studied by real-time NMR kinetics, revealing an alteration of the composition profile of 4MS towards a more block-like structure. Based on the kinetic studies, a series of Myr/I/4MS terpolymers and Myr/S copolymers was prepared by statistical living anionic copolymerisation. All copolymers showed narrow molecular weight distributions (SEC) and two glass transition temperatures ($T_{g,1}$ = -51 to -62 °C; $T_{g,2}$ = 93 to 107 °C), suggesting phase segregation. TEM and SAXS measurements revealed highly ordered lamellar morphologies for all copolymers with long range correlation and confirmed the block-like structure and behaviour of Myr/S and Myr/4MS copolymers prepared by statistical carbanionic copolymerisation.

Induction

ABA triblock copolymers based on inexpensive petroleum based monomers like isoprene (I), butadiene (B) and styrene (S) are highly established and utilized in various applications ranging from footwear to asphalt modifiers.[1] The respective, well-defined block copolymers are predominantly prepared by living anionic copolymerisation using sequential monomer addition steps. Unlike other polymerisation techniques, carbanionic polymerisation does not show termination or transfer steps and thus provides the highest possible level of molecular weight control. This also leads to low dispersity (Poisson-distribution), which are key features for the preparation of materials with tailor-made properties from vinyl monomers.[2,3]

However, dwindling petrochemical resources and an increasing environmental awareness have motivated the interest for bio-based polymer materials from renewable sources. Among the variety of bio-based monomers, myrcene (Myr) has garnered considerable interest due to its convenient availability and structural similarity to isoprene and butadiene. Myrcene belongs to the class of monoterpenes and can be found in many plants like conifers, wild thyme and hops.[4,5] Commercially, myrcene is generated on large scale by pyrolysis of *β*-pinene, and recent developments in metabolic engineering also enable the microbial synthesis of myrcene.[5,6] Like its petroleum-derived diene counterparts, myrcene can be polymerised by various polymerisation techniques like emulsion polymerisation, controlled and free radical polymerisation and living anionic polymerisation.[7–10] To date, the carbanionic statistical copolymerisation of myrcene has only been studied in a few works that lack in-depth kinetic studies.[9,11–13] To explore the potential of myrcene as a comonomer for styrenic copolymers and to establish its applicability for carbanionic copolymerisation, it is indispensable to investigate the copolymerisation kinetics of myrcene.

[a.] Institute of Organic Chemistry, Johannes Gutenberg University, Duesbergweg 10-14, 55128 Mainz, Germany

[b.] Graduate School Materials Science in Mainz, Staudinger Weg 9, 55128 Mainz, Germany

[c.] Macromolecular Chemistry Department, Technische Universität Darmstadt, Alarich-Weiss Str. 4, 64287 Darmstadt, Germany

[d.] Durham Centre for Soft Matter, Department of Chemistry, Durham University, DH1 3LE Durham, United Kingdom

[e.] Department of Physics, University of Ioannina, P.O. Box 1186, 45110 Ioannina, Greece

[f.] Max Planck Institute for Polymer Research, 55128 Mainz, Germany

ARTICLE   **Journal Name**

Previous studies by Quirk et al. and Bolton et al. have shown that myrcene can be copolymerised with styrene. Polymyrcene
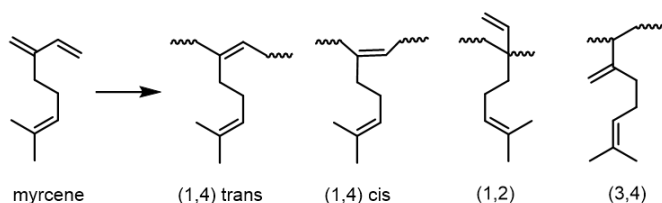

Fig. 1 Structure of myrcene (left) and possible microstructures of polymyrcene.

provides similar properties to polyisoprene, such as a low $T_{g,Myr}$ (- 65 °C) and high content of 1,4 units when polymerised in nonpolar solvents (**Fig. 1**).[9,11,12] Regarding the possible structures shown in **Fig. 1**, we emphasize that the actual incorporation mode is 4,1 trans and 4,1 cis, since the carbanionic chain end attacks preferentially the more reactive 3,4 double bond. Besides sequential monomer addition, the statistical anionic copolymerisation is a very important synthetic strategy to prepare tough materials and to tune material properties.[14–17]

In particular the statistical living anionic copolymerisation of styrene/isoprene and styrene/butadiene is highly relevant for commercial applications and have been extensively studied. [17–20] The importance of these monomer combinations arises from the special kinetics of styrenic and diene monomers. In nonpolar solvents dienes show much higher reactivity than styrenic monomers, resulting in a highly preferred homopolymerisation of the diene monomer and a considerably faster cross-over reaction from a styrenic living chain end to the diene carbanion than the reversed cross-over process.[21,22] Consequently, the incorporation of the diene monomer is highly favoured, yielding tapered copolymers with almost pure diene and styrenic blocks in the polymer chains and a mixed midblock.[23,24] Altering the shape and length of this tapered mid-section has an impact on the mechanical response, i.e., the composition profile is an important "setting screw" for the mechanical properties.[25–28] Understanding the kinetics of a monomer system permits the prediction and tuning of the composition profile and therefore enables the tailoring of the mechanical characteristics. Recent studies by Yang et al. and by our group revealed a high sensitivity of the living anionic copolymerisation kinetics towards even small changes of the electron density of the polymerizable double bond, induced by alkyl substituents at the phenyl ring of styrene.[17,29] Hence, it can be assumed that the inductive effect of the large alkyl substituent of myrcene will affect its copolymerisation behaviour compared to isoprene and butadiene.

To the best of our knowledge, no kinetic studies on the statistical copolymerisation of myrcene have been carried out to date. In this study, we present in-depth kinetics of different copolymerisations of myrcene in nonpolar solvents as well as a detailed characterisation of the resulting myrcene-containing copolymers. For this purpose, the copolymerisations Myr/I; Myr/S; Myr/4MS and the terpolymerisation Myr/I/4MS were monitored by *in-situ* ^{1}H NMR kinetics in cyclohexane, allowing the calculation of the reactivity ratios and composition profiles

of each monomer combination. The results revealed a gradient structure for Myr/I copolymers and block-like composition profiles for Myr/S; Myr/4MS and Myr/I/4MS copolymers, indicating the formation of tapered block copolymers in one step. To confirm the composition profiles, several Myr/S; Myr/4MS and Myr/I/4MS copolymers were prepared by simultaneous copolymerisation and subsequently characterised by SEC, DSC, SAXS and TEM. All copolymers showed low dispersity and well-defined, phase-separated morphologies, confirming the blocky character of these copolymers.

Experimental Section

Materials

All chemicals and solvents were purchased from Acros Organics Co. and Sigma-Aldrich Co. Isopropyl alcohol and methanol were used as received without further purification. Cyclohexane was purified via distillation over sodium and degassed by three freeze-thaw cycles prior to use. Myrcene, isoprene, styrene and 4-methylstyrene were purified by distillation over CaH_2 and degassed by three freeze-thaw cycles prior to use.

Instrumentation

NMR spectra were recorded on a Bruker Avance II 400 spectrometer working 400 MHz (^{1}H NMR). NMR chemical shifts are referenced relative to tetramethylsilane. Standard SEC was performed with THF as the mobile phase (flow rate 1 mL min-1) on a SDV column set from PSS (SDV 10^3, SDV 10^5, SDV 10^6) at 30 °C. Calibration was carried out using PS standards (from Polymer Standard Service, Mainz). For determination of the thermal properties of the polymers, differential scanning calorimetry (DSC) was performed with a Mettler Toledo DSC-1 in a temperature range from -100 °C to 150 °C with a heating rate of 10 K min-1

TEM Measurements

TEM experiments were carried out on a Zeiss EM 10 electron microscope operating at 60 kV. All shown images were recorded with a slow-scan CCD camera obtained from TRS (Tröndle) in bright field mode. Camera control was computer-aided using the ImageSP software from TRS.

SAXS Measurements

Small-angle (SAXS) measurements were made using CuKα radiation (RigakuMicroMax 007 x-ray generator, Osmic Confocal Max-Flux curved multilayer optics). 2D diffraction patterns were recorded on an Mar345 image plate detector at a sample-detector distance of 2289 mm. Intensity distributions as a function of the modulus of the total scattering vector, $q = (4\pi/\lambda) \sin(2\theta/2)$, where 2θ is the scattering angle, were obtained by radial averaging of the 2D datasets. Samples in the form of thick films (~1 mm) were prepared by slow solvent casting (chloroform). Measurements of 1 hour duration were made at 298 K.

Journal Name ARTICLE

^{1}H-NMR kinetics studies

The monomer/solvent mixtures (20 wt% in cyclohexane-d_{12}) were prepared in a glove box. All compounds were purified via distillation over CaH$_2$ prior to use. The mixtures were filled in conventional NMR tubes and sealed with rubber septa. A NMR spectrum of the mixture was measured prior to the initiation step. After the initiation with one drop of *sec*-butyllithium (1.3 M in cyclohexane/hexane 92/8) the NMR experiments were started without locking and shimming of the polymerization mixture. All spectra were measured with 4 scans at 400 MHz and a time interval of 20 seconds between the spectra. The reaction temperature was kept constant at 23 °C. Typically, 150-250 ^{1}H NMR spectra were and evaluated.

Determination of reactivity ratios and microstructure

To determine the reactivity ratios, the proton signals 5.54-5.64 ppm (4MS), 5.6-5.7 ppm (S), 6.29-6.37 ppm (Myr) and 6.34-6.44 (I) were used. Data from the copolymerisation experiments were fitted to both the ideal, nonterminal model ($r_1 \cdot r_2 = 1$) and the terminal model Model (Mayo-Lewis).[30] The ideal model was fitted by an equation recently reported (see Table S1, entry 3, Supp. Inform.).[31,32] The Mayo-Lewis model in its integrated form, i.e., the Meyer-Lowry equation, was used to fit the terminal model. The experimental data can be sufficiently described by the non-terminal model. The reactivity ratios determined by the *in-situ* method were therefore used to simulate the gradient structure of the co- and terpolymerisation. The procedures are explained in detail in the Supporting Information.

General polymerization procedure for myrcene co-polymerisations

All copolymerisations were carried out in cyclohexane in an argon atmosphere and at room temperature in a glove-box in 30 ml glass flasks equipped with septa. The degassed monomer/ solvent (20 wt%) was initiated with *sec*-butyllithium (1.3 M in cyclohexane/hexane 92/8) via syringe. The solution was stirred over night to ensure full monomer conversion. The polymerization was terminated by adding 0.5 ml of degassed isopropyl alcohol by a syringe. The polymers were precipitated in a large excess of isopropanol, dried at reduced pressure and stored at -18 °C.
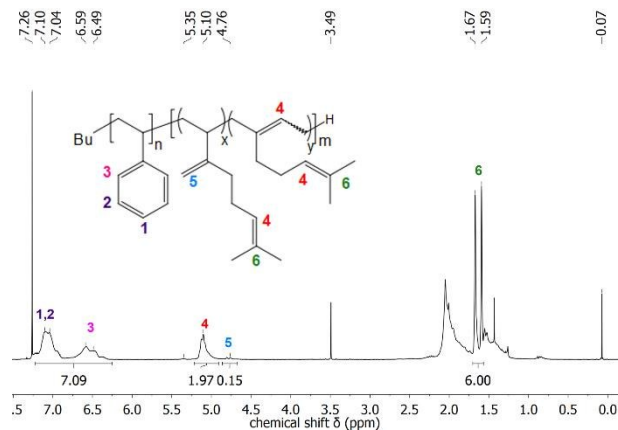

Fig. 2 ^{1}H NMR spectrum of copolymer Myr$_{0.42}$-S$_{0.58}$ (Table 1 Entry 7) in CDCl$_3$ at 23 °C.

Results and discussion

Microstructure analysis

Like polyisoprene and polybutadiene, polymyrcene shows a high content of 1,4 units (95%) and a low percentage of 3,4 units (5%), when polymerised in non-polar solvents (**Fig. 2**). The formation of 1,2 units was not observed, which can be
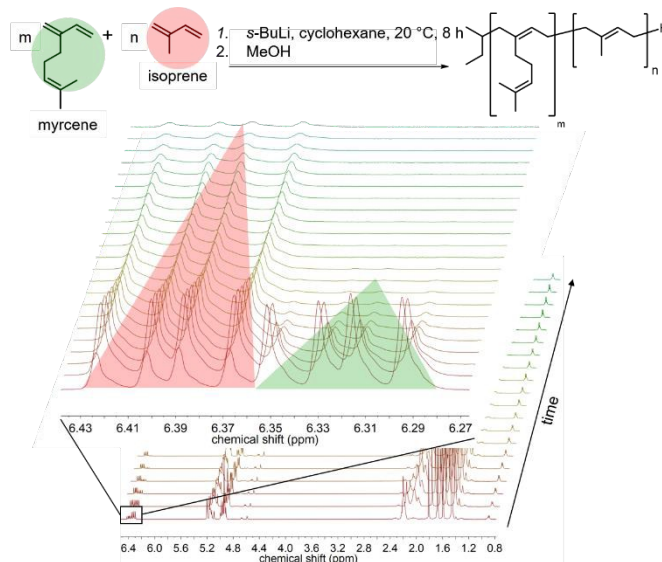

Fig.3 Reaction conditions of the *in-situ* NMR kinetics experiment (top) and in-situ monitoring of decreasing monomer signals by real time ^{1}H NMR spectroscopy.

explained by the steric hindrance of this double bond. The double bond of the alkyl side chain remains inactive throughout the carbanionic polymerisation of myrcene, providing a high density of dangling double bonds, which can be used for a variety of post-modification reactions without affecting the 1,4 backbone microstructure.[13,33]

In situ ^{1}H NMR kinetic studies of myrcene

To investigate the copolymerisation kinetics of myrcene, copolymerisation experiments with isoprene, styrene and 4-methylstyrene, respectively were carried out and monitored by real time ^{1}H NMR spectroscopy (**Fig.**). The corresponding kinetic curves and evaluations are given in Figures S8-S10 and S1-S3, Supp. Inform., respectively.

Following the decrease of the specific monomer signals permits the calculation of the reactivity ratios of each monomer combination. The experimental data could be adequately described with the ideal, nonterminal copolymerization model first described by Wall.[34] The explanatory power (R²) did not increase significantly for the more elaborated Mayo-Lewis terminal model. To avoid overfitting, the ideal model was used exclusively to determine the reactivity ratios (a more detailed explanation of the methods can be found in the Supporting Information). This model can also be directly applied to describe the terpolymeri-sation. In a second step, the reactivity ratios were used to simulate the composition profiles of each monomer combination (**Fig. 4**) (a detailed explanation is given in Supp. Inform. Figures S4-S7 and equations 1-12). For a better comparison of the composition profiles, all simulations are

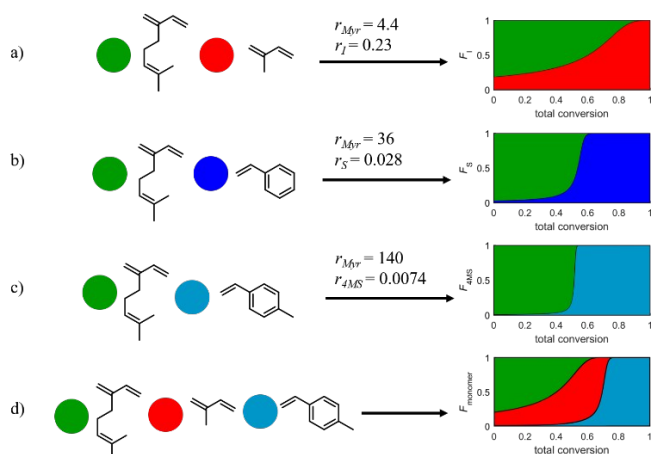given at equimolar monomer ratios. In the statistical copolymerisation of myrcene and isoprene, myrcene was

Fig. 4 Simulated composition profiles of myrcene co- and terpolymers.

consumed faster, which is due to the rapid cross-over reaction from polyisoprenyllithium to polymyrcenyllithium in comparison to crossover vice versa (r_{Myr} = 4.4 ± 0.02; r_I = 0.23 ± 0.0008). The resulting gradient copolymer showed a weakly tapered composition profile with a gradual increase of the isoprene content at higher conversion (**Fig. 4 a**). Similar reactivity ratios were observed for the copolymerisation of isoprene and butadiene in nonpolar solvents (r_I = 3.6; r_B = 0.5).[35] For both monomer combinations, the electron donating effect of the alkyl substituent of isoprene and myrcene is likely responsible for the slightly increased monomer reactivities. The reactivity can be correlated to the strength of the electron donating effect, with a correlation between electron density of the double bond and the reactivity of the diene monomer.

Turning to the copolymerisation of myrcene with styrene and 4-methylstyrene, the formation of block-like composition profiles with almost pure diene and styrenic blocks and a very short and steep gradient was observed (**Error! Reference source not found.4 b** and **c**). The block-copolymer like structure is very pronounced for Myr/4MS copolymers and can be attributed to the vigorously different reactivities (r_{Myr} = 140 ± 9; r_{4MS} = 0.0074 ± 0.0005). This tremendous disparity of the reactivity ratios can again be explained by the electron donating effect of the alkyl substituents. The impact of the electron density at the double bond of a monomer has opposite effects on the monomer reactivity and the reactivity of the carbanionic living chain end of the respective monomer. During anionic polymerisation, the monomer addition step involves a nucleophilic attack of the carbanion chain end on the monomers' double bond. Enhancing the electron density at the double bond lowers its electrophilicity and therefore its reactivity towards a nucleophilic attack.[36,37] On the other hand, an increased electron density enhances the nucleophilicity of the living chain end, resulting in a higher reactivity.[29] In the case of 4-methylstyrene, the electron releasing effect of the methyl group deactivates the vinyl group to nucleophilic attacks and yet makes the propagating site more nucleophilic.

Since there is only one vinyl group, the effect is felt strongly by both monomer and propagating chain end. However, this is not the case for myrcene. Due to its asymmetric structure, myrcene´s double bonds are affected unequally by the electron releasing effect of the alkyl group. The proximity of the 1,2 double bond to the alkyl group makes it more nucleophilic than the 3,4 double bond, directing the propagating chain end to attack the more electrophilic 3,4 double bond. As a result, when myrcene is the propagating unit, the active site is directly impacted by the adjacent, electron donating alkyl substituent, making the carbanion even more nucleophilic. This results in a highly favoured homo-polymerisation of myrcene and very fast cross-over reaction from poly-4-methylstyryllithium to polymyrcenyllithium. The opposite cross-over reaction as well as the homopolymerisation of 4MS are less favoured and much slower. This results in high ratios of cross-over and
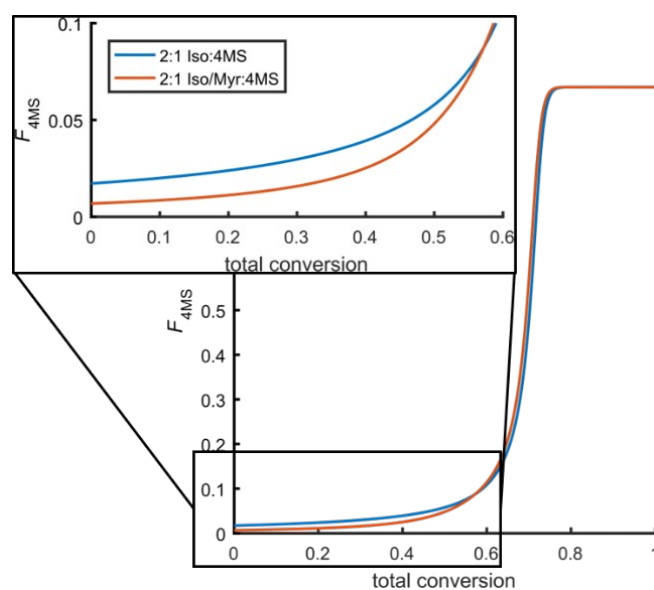

Fig. 5 Simulated composition profile of 4-methylstyrene in a statistical copolymerisation of I/4MS (blue) and a statistical terpolymerisation of Myr/I/4MS (red). For a better comparison of the composition profiles the region at a total conversion from 0 to 60 % was magnified.

homopolymerisation rates, permitting the formation of strongly block-like, tapered copolymers in one step.

In the case of myrcene and styrene, this effect is less pronounced, due to the lower electron density of styrene´s vinyl group as compared to 4-methylstyrene. This results in a higher monomer reactivity than for 4MS and therefore a more favoured incorporation of styrene. The resulting composition profile is very similar to the composition profile of I/4MS,[18] since both monomer systems possess similar reactivity ratios (r_{Myr} = 36 ± 0.3; r_S = 0.028 ± 0.0003 and r_I = 25.4; r_{4MS} = 0.07).[17] Compared to copolymers from Myr/4MS, Myr/S copolymers exhibit a longer tapered section and a higher content of styrene units in the diene section, yielding a less blocky structure than Myr/4MS. It can be assumed that the longer taper will affect the physicochemical properties and the phase segregation behaviour due to its compatibilising effect.[17]

Journal Name
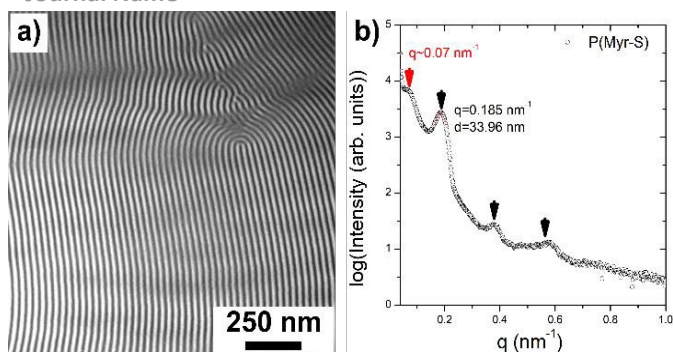
Fig. 6 a) TEM image from the bulk morphology characterization for the polymer $Myr_{0.42}$-$S_{0.58}$. Thin section microtomed at -80 °C with 50 nm thickness, the sample was annealed at 130 °C for 24 hours. PMyr domain were stained with OsO_4. b) SAXS pattern for the sample $Myr_{0.42}$-$S_{0.58}$. Arrows give the position of the Bragg reflections corresponding to a lamellar morphology.

In a recent study, Hutchings et al. demonstrated the impact on the composition profile of B/S by the addition of 1,1-diphenylethylene (DPE).[38] The statistical terpolymerisation of B/S/DPE yielded more block-like structures than statistical B/S copolymers, which can be attributed to a significant change of the B/S copolymerisation kinetics induced by DPE. In order to investigate whether a similar effect can be achieved for I/4MS copolymers, a terpolymerisation of Myr/I/4MS was carried out and monitored by *in situ* NMR spectroscopy (**Error! Reference source not found. d** and Figures S4-S7, Supp. Inform.). A direct comparison of the composition profiles of statistical copolymers of I/4MS and Myr/I/4MS reveals only minor differences (**Fig.**). However, the addition of myrcene to the copolymerisation of I/4MS lowers the content of 4MS repeat units in the diene section, resulting in a higher "structural homogeneity" of the diene block, providing a more block-like structure.

Thermal behaviour

To investigate the influence of the composition profile on the thermochemical properties, a series of myrcene copolymers was prepared by statistical carbanionic copolymerisation. All polymers showed high molecular weights and narrow molecular weight distributions (Error! Reference source not found.). Our previous studies on block-like tapered copolymers revealed a strong correlation between the shape and length of the tapered section and the glass transition temperatures of the individual segments.[17,39] Due to the compatibilizing effect of the gradient, a long tapered section results in the approach of both glass transitions. A short taper, the tapered copolymers virtually indistinguishable from a perfect diblock copolymer. This correlation was also observed for this series of myrcene copolymers. The kinetic studies revealed a slightly more pronounced gradient for Myr/S copolymers than for Myr/4MS copolymers. Consequently, the $T_{g, Myr}$ of $Myr_{0.42}$-$S_{0.58}$ (Entry 7, Table 1) is higher than $T_{g, Myr}$ of $Myr_{0.5}$-$4MS_{0.5}$ (Entry 6, Table 1), due to the lower purity of the myrcene segment of $Myr_{0.42}$-$S_{0.58}$. The slightly longer taper of $Myr_{0.42}$-$S_{0.58}$ also has an impact on $T_{g,S}$ and $T_{g,Myr}$, showing small deviations when compared to PS and PMyr homopolymers ($T_{g,S}$ = 100°C, $T_{g,Myr}$ = -65°C). In the case of Myr/I/4MS terpolymers the low

T_g from DSC was very broad suggesting the presence of different segmental mobilities of I and Myr.

Entry	Sample composition [a] (mol%)	M_n [b] (kg/mol)	$Đ$ [b]	$T_{g,1}$ [c] (°C)	$T_{g,2}$ [c] (°C)
1	$I_{0.5}$-$4MS_{0.5}$	64.1	1.07	-51	103
2	$Myr_{0.1}$-$I_{0.4}$-$4MS_{0.5}$	67.0	1.08	-53	106
3	$Myr_{0.2}$-$I_{0.3}$-$4MS_{0.5}$	65.9	1.08	-57	107
4	$Myr_{0.3}$-$I_{0.2}$-$4MS_{0.5}$	71.5	1.09	-59	101
5	$Myr_{0.4}$-$I_{0.1}$-$4MS_{0.5}$	64.0	1.12	-61	102
6	$Myr_{0.5}$-$4MS_{0.5}$	63.8	1.14	-62	107
7	$Myr_{0.42}$-$S_{0.58}$	49.4	1.04	-54	93
8	$Myr_{0.26}$-$S_{0.74}$	161.5	1.04	-52	107

[a] **Table 1.** Summarized results of NMR, SEC, DSC, TEM and SAXS characterisation of myrcene copolymers. determined by ^{1}H NMR spectroscopy in $CDCl_3$; [b] determined by SEC in THF at 30 °C; [c] determined by DSC at 10 K/min

Furthermore, the kinetics studies indicated an alteration of the composition profile of I/4MS in the terpolymer towards a more block-like structure, induced by the addition of myrcene. To verify this observation, a series of terpolymers with a targeted molecular weight of 60 kg/mol and a constant 4MS content but varying contents of I and Myr (Table 1 Entries 1-6) was prepared and examined by SEC and DSC. In all cases a slightly higher molecular weight was observed, which can be mainly attributed to the calibration with polystyrene standards. In addition, a slight increase of the dispersity with increasing content of myrcene was observed for samples 2 to 6 (Error! Reference source not found.).

A tentative explanation for the higher dispersity values is based on the very slow cross over reaction from polymyrcenyllithium to 4MS, which translates to inhomogeneous initiation, resulting in a higher dispersity of the 4MS segments. All terpolymers showed two T_gs, clearly indicating the presents of a mixed Myr/I and a pure 4MS segment ($T_{g,I}$ = -65°C $T_{g,4MS}$ = 106°C), which is in good agreement with the results of the *in-situ* NMR kinetic measurements. The alteration of the myrcene content of the terpolymers showed only minor changes of $T_{g, 4MS}$. At the same time a significant decrease of the T_g the mixed Myr/I section for an increasing myrcene content was observed, when compared to a corresponding I/4MS copolymers (Table 1, Entries 1-5). These results may be explained by the enhancement of the block character induced by the addition of myrcene, verifying the observations of the real time NMR kinetic studies.

Phase segregation behaviour

The existence of two discrete glass temperatures for all copolymers prepared by statistical anionic copolymerization in nonpolar solvents hints at phase segregation, however even miscible systems may exhibit two T_gs. Phase segregation depends not only on the difference in reactivity ratios, but also on the product of the interaction parameter between unlike segments with the total degree of polymerization. To verify

ARTICLE

Journal Name

these findings, the morphologies of four statistical block copolymer samples were investigated by TEM and SAXS measurements at ambient temperature (Supp. Inf., Figures S16-S25). For this purpose, bulk characterization was accomplished after solvent evaporation of the block copolymers in chloroform or tetrahydrofuran, followed by thermal annealing at 130 °C in a nitrogen atmosphere for 24 hours. The polymer films were cut into thin slices of 50-70 nm by ultramicrotomy and the collected thin slices were stained with osmium tetroxide, OsO_4, for selective staining of the PI-
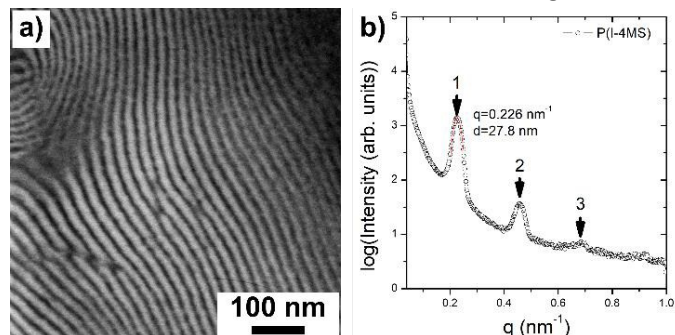
Fig. 7 a) TEM image from the bulk morphology characterization for the polymer $I_{0.5}$-$4MS_{0.5}$. A thin section was microtomed at -80 °C with 50 nm thickness. The sample was annealed at 130 °C for 24 hours. PMyr domains appear dark and were stained with OsO_4. b) SAXS pattern for the sample $I_{0.5}$-$4MS_{0.5}$. Arrows give the positions of the Bragg reflections corresponding to a lamellar morphology

and PMyr-containing domains. In **Figure 6**, a corresponding TEM image of sample $Myr_{0.42}$-$S_{0.58}$ (Table 1, Entry 7) after staining is given, revealing a lamellar morphology with lamellar periods, that is, the distance of two lamellae, of about 30.7 nm. To gain more insights into the microphase separated structure, SAXS measurements of the sample $Myr_{0.42}$-$S_{0.58}$ was carried out. The corresponding SAXS pattern is shown in **Figure 6 b** revealing several pronounced diffraction peaks with positions 1:2:3 relative to the first peak, corresponding to a lamellar morphology. The periodicity of the lamellar structure from SAXS (obtained as $d=2\pi/q^*$, q^* is the modulus of the scattering vector corresponding to the first peak) is $d = 34.0$ nm, in good agreement with TEM measurements. The diffraction peak at q = 0.07 nm is tentatively explained by partial crosslinking caused by prolonged thermal annealing
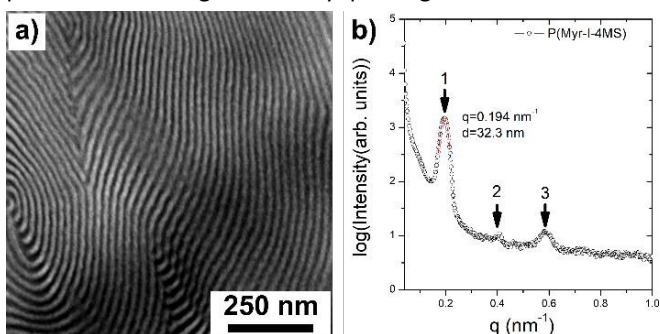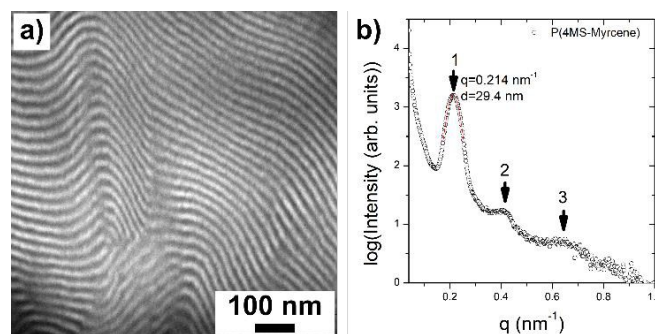

Fig. 8 a) TEM image from the bulk morphology characterization for the polymer $Myr_{0.2}$-$I_{0.3}$-$4MS_{0.5}$. Thin section microtomed at -80 °C with 50 nm thickness, the sample was annealed at 130 °C for 24 hours. PMyr domains were stained with OsO_4. b) SAXS pattern for the sample $Myr_{0.2}$-$I_{0.3}$-$4MS_{0.5}$. Arrows give the positions of the Bragg reflections corresponding to a lamellar morphology

during sample preparation.

In **Figure 7**, a TEM image of sample $I_{0.5}$-$4MS_{0.5}$ (Table 1, Entry 1) after staining with OsO_4 is given, revealing a lamellar morphology with a lamellar period of 24.4 nm. Additionally the SAXS pattern is also shown in **Figure 7 b,** displaying Bragg reflections with positions 1:2:3 relative to the first peak of a lamellar structure with a lamellar thickness of $d = 27.8$ nm, in accordance with the TEM measurements.

In **Figure 8**, a TEM image of sample $Myr_{0.2}$-$I_{0.3}$-$4MS_{0.5}$ (Table 1 Entry 3) after staining with OsO_4 is given, revealing a

Fig. 9 a) TEM image from the bulk morphology characterization for the polymer $Myr_{0.5}$-$4MS_{0.5}$. Thin section microtomed at -80 °C with 50 nm thickness, the sample was annealed at 130 °C for 24 hours. PMyr domains were stained with OsO_4. b) SAXS pattern for the sample $Myr_{0.5}$-$4MS_{0.5}$. Arrows give the position of the Bragg reflections corresponding to a lamellar morphology.

lamellar morphology with a lamellar period of 30.1 nm. Additionally the SAXS pattern is also shown in Figure 8, again showing Bragg reflections with positions 1:2:3 relative to the first peak of the lamellar structure with a periodicity of $d = 32.3$ nm. Again, these results are in good agreement with TEM measurements. Furthermore, the morphology of sample $Myr_{0.5}$-$4MS_{0.5}$ (Table 1 Entry 6) was investigated. Exemplarily, a TEM image after staining with OsO_4 is shown in **Figure 9** revealing a lamellar morphology with a lamellar period of 28.7 nm. Additionally, confirmation is given by the SAXS pattern shown in **Figure 9 b**, which translates to a periodicity of $d = 29.4$ nm.

All four tapered block copolymers generated by statistical anionic copolymerization in nonpolar solvents show excellent phase-segregated domains and a lamellar morphology as expected from the composition. The domain sizes obtained by TEM and SAXS measurements are summarised in **Table 2**. Furthermore, this general synthetic approach is also suitable for the preparation of bio-based high molecular weight copolymers in one step (Table 1 Entry 8). Corresponding to its composition, $Myr_{0.26}$-$S_{0.74}$ shows a well-defined asymmetric lamellar morphology and large domain sizes (Supp. Inf. **Figure S20 and S25**).

Entry	Sample composition (mol%)	d_{TEM} (nm)	d_{SAXS} (nm)
1	$I_{0.5}$-$4MS_{0.5}$	24.4	27.8
2	$Myr_{0.2}$-$I_{0.3}$-$4MS_{0.5}$	30.1	32.3
3	$Myr_{0.5}$-$4MS_{0.5}$	28.7	29.4
4	$Myr_{0.42}$-$S_{0.58}$	30.7	34.0

Polymer Chemistry Accepted Manuscript

Please do not adjust margins
Polymer Chemistry

ARTICLE

Table 2. Lamellar periods obtained from TEM and SAXS measurements.

Conclusions

The statistical anionic copolymerisation of the terpene-mono-mer myrcene with isoprene, styrene and 4-methylstyrene, respectively has been extensively studied by real time ^{1}H NMR spectroscopy during copolymerisation. Following the monomer consumption directly leads to a detailed under-standing of the composition profiles of the resulting copolymers in the living copolymerization and permits calculation of reactivity ratios for each monomer combination. For all monomer combinations, myrcene was consumed significantly faster than the respective comonomers, yielding strongly tapered composition profiles. This effect was especially pronounced in the copolymerisations of Myr/S and Myr/4MS. Both combinations showed highly disparate reactivity ratios, resulting in block-like structures with almost pure polydiene and pure styrenic blocks, separated by short and steep gradients. Furthermore, kinetic studies of the terpolymerisation of Myr/I/4MS revealed an alteration of the composition profile of 4MS towards a more block-like structure, when compared to a corresponding I/4MS copolymer. To verify the blocky character of these copolymers, several Myr/4MS and Myr/S copolymers and a series of Myr/I/4MS terpolymers with varying Myr/I content were prepared by direct, i.e., statistical carbanionic copolymerisation. All samples showed two distinct glass transitions, with values corresponding to the homopolymers confirming the (tapered) block-like character of these copolymers. This conclusion is also supported by TEM and SAXS measurements, showing that all samples exhibit microphase separation and form lamellar morphologies with long range order. All these findings clearly demonstrate the high potential of the bio-based monomer myrcene for the carbanionic one-step synthesis of block-like copolymers, which is a key feature when targeting bio-based thermoplastic elastomers or tapered multiblock architectures.[40]

Conflicts of interest

There are no conflicts to declare.

Acknowledgements

References

View Article Online
DOI: 10.1039/C8PY01711E

1. C. M. Bates and F. S. Bates, *Macromolecules*, 2017, **50**(1), 3.
2. A. Natalello, J. N. Hall, E. A. L. Eccles, S. M. Kimani and L. R. Hutchings, *Macromol. Rapid Commun.*, 2011, **32**(2), 233.
3. L. R. Hutchings, P. P. Brooks, D. Parker, J. A. Mosely and S. Sevinc, *Macromolecules*, 2015, **48**(3), 610.
4. P. Sarkar and A. K. Bhowmick, *RSC Adv.*, 2014, **4**, 61343.
5. A. Behr and L. Johnen, *ChemSusChem*, 2009, **2**(12), 1072.
6. E.-M. Kim, J.-H. Eom, Y. Um, Y. Kim and H. M. Woo, *J. Agric. Food. Chem.*, 2015, **63**(18), 4606.
7. P. Sarkar and A. K. Bhowmick, *ACS Sustainable Chem. Eng.*, 2016, **4**(10), 5462.
8. A. Métafiot, Y. Kanawati, J.-F. Gérard, B. Defoort and M. Marić, *Macromolecules*, 2017, **50**(8), 3101.
9. A. Ávila-Ortega, M. Aguilar-Vega, M. I. Loría Bastarrachea, C. Carrera-Figueiras and M. Campos-Covarrubias, *J. Polym. Res.*, 2015, **22**(11), 8.
10. K. Satoh, *Polym. J.*, 2015, **47**(8), 527.
11. J. M. Bolton, M. A. Hillmyer and T. R. Hoye, *ACS Macro Lett.*, 2014, **3**(8), 717.
12. R. P. Quirk, *US Patent 4374957 A*(4374957 A), 1983.
13. A. Matic and H. Schlaad, *Polym. Int.*, 2018, **67**(5), 500.
14. K. Knoll and N. Nießner, *Macromol. Symp.*, 1998, **132**(1), 231.
15. M. A. Morris, T. E. Gartner and T. H. Epps, *Macromol. Chem. Phys.*, 2017, **218**(5), 1600513.
16. R. Roy, J. K. Park, W.-S. Young, S. E. Mastroianni, M. S. Tureau and T. H. Epps, *Macromolecules*, 2011, **44**(10), 3910.
17. E. Grune, T. Johann, M. Appold, C. Wahlen, J. Blankenburg, D. Leibig, A. H. E. Müller, M. Gallei and H. Frey, *Macromolecules*, 2018, **51**(9), 3527.
18. H. L. Hsieh, *J. Polym. Sci., Part A: Polym. Chem.*, 1965, **3**(1), 163.
19. S. Bywater and D. J. Worsfold, *J. Phys. Chem.*, 1966, **70**(1), 162.
20. L. J. Fetters, N. P. Balsara, J. S. Huang, H. S. Jeon, K. Almdal and M. Y. Lin, *Macromolecules*, 1995, **28**(14), 4996.
21. D. J. Worsfold, *J. Polym. Sci., Part A: Polym. Chem.*, 1967, **5**(11), 2783.
22. H. L. Hsieh and W. H. Glaze, *Rubber Chem. Technol.*, 1970, **43**(1), 22.
23. Y. Tsukahara, N. Nakamura, T. Hashimoto, H. Kawai, T. Nagaya, Y. Sugimura and S. Tsuge, *Polym. J.*, 1980, **12**(7), 455.
24. T. Hashimoto, Y. Tsukahara, K. Tachi and H. Kawai, *Macromolecules*, 1983, **16**(4), 648.
25. P. Hodrokoukes, G. Floudas, S. Pispas and N. Hadjichristidis, *Macromolecules*, 2001, **34**(3), 650.
26. P. Hodrokoukes, S. Pispas and N. Hadjichristidis, *Macromolecules*, 2002, **35**(3), 834.
27. S. E. Mastroianni and T. H. Epps III, *Langmuir*, 2013, **29**(12), 3864.
28. M. Luo, J. R. Brown, R. A. Remy, D. M. Scott, M. E. Mackay, L. M. Hall and T. H. Epps, *Macromolecules*, 2016, **49**(14), 5213.
29. L. Yang, H. Ma, L. Han, P. Liu, H. Shen, C. Li and Y. Li, *Macromolecules*, 2018, **51**(15), 5891.
30. F. R. Mayo and F. M. Lewis, *JACS*, 1944, **66**(9), 1594.
31. V. E. Meyer and G. G. Lowry, *J. Polym. Sci. A Gen. Pap.*, 1965, **3**(8), 2843.
32. J. Blankenburg, E. Kersten, K. Maciol, M. Wagner, S. Zarbakhsh and H. Frey, *to be submitted*.
33. C. Zhou, Z. Wei, C. Jin, Y. Wang, Y. Yu, X. Leng and Y. Li, *Polymer*, 2018, **138**, 57.
34. F. T. Wall, *J. Am. Chem. Soc.*, 1941, **63**(7), 1862.
35. H. L. Hsieh and R. P. Quirk, *Anionic Polymerization: Principles and Practical Applications*, Chapman and Hall/CRC, Boca Raton, 1996.
36. K. S. Dhami and J. B. Stothers, *Can. J. Chem.*, 1965, **43**(2), 479.
37. T. Ishizone, A. Hirao and S. Nakahama, *Macromolecules*, 1993, **26**(25), 6964.
38. L. R. Hutchings, P. P. Brooks, P. Shaw and P. Ross-Gardner, *J. Polym. Sci. A Polym. Chem.*, 2019, 57 (3), 382.
39. M. Appold, E. Grune, H. Frey and M. Gallei, *ACS Appl. Mater. Interfaces*, 2018, **10**(21), 18202.
40. M. Steube, T. Johann, E. Galanos, M. Appold, C. Rüttiger, M. Mezger, M. Gallei, A. H.E. Müller, G. Floudas, H. Frey, *Macromolecules,* 2018, **51**, 10246.

Polymer Chemistry Accepted Manuscript

Please do not adjust margins